

# Filtration of Paint-Contaminated Water by Electrospun Membranes

Ann-Kathrin Müller, Zhi-Kang Xu, and Andreas Greiner\*

Micro- and nanosized plastics as persistent anthropogenic pollutants have attracted more and more attention in recent years. A source of nanoparticles is, for example, water-borne dispersion paint, which consists of a variety of different materials with potential adverse effects on living systems. Therefore, a rising challenge becomes apparent to investigate remediation strategies for environmental media. This problem is addressed by utilizing electrospun membranes for filtration applications because of their outstanding properties, such as their high surface-to-volume ratio and ease of functionalization. The electrospun membranes are able to successfully filter different paint components, such as titanium dioxide and polyacrylate nanoparticles, as well as dispersed polymers and calcium carbonate microparticles. Besides the known size-exclusion mechanism, the membranes featured extraordinary properties, such as effective separation of components smaller than the pore size of the electrospun membranes. This property occurs due to the fiber surface functionalization and enables not only filtration of nanosized or dissolved mater at high filtration efficiencies up to 100% but also at a very low operating pressure. This combination of filter material properties cannot be achieved by conventional nanofiltration membranes and thus, demonstrates the high potential of electrospun membranes for the application in filtration for future environmental pollutants.

## 1. Introduction


In recent decades, the establishment of nanomaterials led to the rapid development of the economic sector and the implementation of nanomaterials in diverse products.<sup>[1]</sup> Nanoparticles (NPs) as part of nanomaterials feature particle sizes below 1000 nm<sup>[2]</sup> and can be made of metal or polymer materials. Both metal NPs and nanoplastics are currently attracting attention due to their unique properties and their still unknown impacts on the environment and human health. The potential impacts of metal NPs and nanoplastics have been deeply investigated in recent years since the human body is exposed to metal NPs and nanoplastics via diet, arising the thread of bioaccumulation in food webs.<sup>[3]</sup> Metal NPs and nanoplastics can induce the activation of a cell-response in different biological systems<sup>[4–7]</sup> up to human beings.<sup>[8–10]</sup> Adverse effects in vivo include: inflammation, production of reactive oxygen species, or cytotoxicity.<sup>[11, 12]</sup>

Paints from buildings and road markings are a source of metal and metal oxide NPs<sup>[13]</sup> and plastic particles.<sup>[14,15]</sup> It is estimated that roughly 10–30% of titanium dioxide NPs production was used for paints and/or related products.<sup>[16]</sup> Since external surfaces of buildings and road markings are exposed to weathering, paint erosion occurs.<sup>[17,18]</sup> Weathering elements cause paint matrix degradation which is dependent on the painted materials, the nature of contact,<sup>[19]</sup> the season,<sup>[20]</sup> weathering duration, water pH, rainfall duration and intensity.<sup>[21]</sup> When the paint matrix is degraded, former embedded titanium dioxide NPs are released into the environment by effects of rain, condensed water, wind, and mechanical vibrations.<sup>[22]</sup> In 2008, it was evidenced for the first time that titanium dioxide NPs were found in the environment as a consequence of leaching from paint.<sup>[23]</sup> Quantities of titanium dioxide NPs released from facades might be in the range of  $168 \pm 121 \mu\text{g m}^{-2}$  during seven weeks in the winter.<sup>[20]</sup>

The paint matrix often consists of polymer particles but also secondary plastic particles result from paint degradation, which have been shown to be a significant fraction of microplastic polluting the oceans.<sup>[14,24]</sup> They might arise from the abrasion of ship hulls, road markings, and external surfaces of buildings.<sup>[25]</sup> Novel “green” chemical technologies had been developed to reduce paint fouling by implementing antimicrobial functions.

A.-K. Müller, A. Greiner  
 Macromolecular Chemistry and Bavarian Polymer Institute  
 University of Bayreuth  
 Universitätsstraße 30, 95440 Bayreuth, Germany  
 E-mail: greiner@uni-bayreuth.de

Z.-K. Xu  
 MOE Key Laboratory of Macromolecular Synthesis and Functionalization  
 and Key Laboratory of Adsorption and Separation Materials &  
 Technologies of Zhejiang Province  
 Department of Polymer Science and Engineering  
 Zhejiang University  
 Hangzhou 310027, China

 The ORCID identification number(s) for the author(s) of this article can be found under <https://doi.org/10.1002/mame.202200238>

© 2022 The Authors. Macromolecular Materials and Engineering published by Wiley-VCH GmbH. This is an open access article under the terms of the Creative Commons Attribution License, which permits use, distribution and reproduction in any medium, provided the original work is properly cited.

DOI: 10.1002/mame.202200238

These are based on amphiphilic block copolymers exhibiting tailored surface reactivity, functionality, and reconstruction for antifouling applications.<sup>[26]</sup> An inherent drawback is the non-biodegradability deteriorating plastic problems in the environment.

Metal NPs and nanoplastics released from paints are supposed to end up in municipal wastewater treatment plants, where they had been proven in 2011 for the first time.<sup>[27]</sup> Municipal wastewater treatment plants are often based on degradation by activated sludge, which arose concerns in recent years, since many NPs are known for their toxic effects on microbes.<sup>[28]</sup> Nevertheless, different publications demonstrate that metal oxide NPs and microplastics can be removed from aqueous media with a retention of more than 82%.<sup>[27,29]</sup> Often the sludge is applied as fertilizer to soils, resulting in the discharge of NPs in the environment.<sup>[30]</sup> Wastewaters from paint industry are currently treated by a combination of different processes, such as coagulation/flocculation/membrane filtration, since these are considered as a non-expensive and efficient methods.<sup>[31]</sup> Ultrafiltration was utilized to remove the smallest particles. However, efficiency was often insufficient and very high pressures were needed.<sup>[32]</sup> Recently, the focus on highly efficient purification methods was directed to membrane techniques.<sup>[33]</sup> For example, Wang et al. demonstrated the efficient removal of polystyrene NPs from water by electrospun membranes as model system.<sup>[34]</sup> Additionally, Batool et al. described the batch adsorption of different nanoplastics by electrospun cellulose fibers coated with polyethylene imine.<sup>[35]</sup> However, model NPs might not represent the particle characteristics from commercial sources and might feature a different behavior in water treatments.

In this study, we focus on membrane filtration of paint-contaminated wastewater. Since paints are known to be a NP source polluting the environment with potential adverse effects on biota, an urgent need for purification methods becomes apparent. We address this prospective problem by utilizing electrospun membranes for filtration application. So far publications focused on the filtration of one, in lab synthesized particle or material, with specific material properties. However, this might not represent the conditions, observed in real systems. Here, often mixtures of various materials occur, which might interact with each other and thus, change their original particle properties, for example, surface charge, swelling state of polymer, particle stability, surface functional groups. We chose two different wall paints as real-life examples to get a more realistic insight into the behavior of commercial material mixtures in filtration applications. This work contributes to the understanding of filtration mechanisms of new occurring pollutant mixtures, such as metal and plastic NPs from paints.

## 2. Results and Discussion

### 2.1. Paint Composition and Potential Environmental Hazard

Two commercial walls, respectively, ceiling water-borne dispersion paints were selected as real sources of metal NPs and nanoplastics. The wall paint will be termed paint 1, in contrast to the ceiling paint, which is named as paint 2. In our previous paper, both paint mixtures have been separated into two fractions for each paint. The fractions were termed as supernatant

and sludge and consist of one, pure compound. The size, shape, and composition of the components were analyzed: paint 1 supernatant ( $\approx 200$  nm polyacrylate NPs), paint 1 sludge (50–150 nm titanium dioxide NPs), paint 2 supernatant ( $\approx 800$  nm dispersed copolymer), paint 2 sludge (up to 10  $\mu\text{m}$  calcium carbonate microparticles). Additionally, the toxicity of the compounds was tested on biological systems, such as *Daphnia magna* and cell cultures, demonstrating concentration dependent adverse effects on their vitality. Thus, purification of paint-contaminated surface waters is becoming an important issue.

### 2.2. Membrane Filtration

Electrospun membranes are a versatile module for wastewater purification and can easily be fine-tuned for specialized filtration applications, such as affinity separation.<sup>[36]</sup> Since the paint dispersions possess a negative zeta potential, they can be attracted by a positively charged affinity membrane. The positive charges on the membrane surfaces are provided by a copolymer containing 50 mol% quaternary amine groups as possible adsorption sites for particles. The copolymer was synthesized by free-radical copolymerization and was electrospun and cross-linked under UV light to obtain a membrane with high mechanical stability. The polymer synthesis, electrospinning procedure, and membrane properties have already been reported in our previous publication.<sup>[37]</sup>

The electrospun affinity membrane was tested for filtration of the two paints. The pore size of the membrane was in the range of 1.2–1.7  $\mu\text{m}$  with a fiber diameter of 300–400 nm. The filtration experiments were conducted for the paint dispersion and the paint supernatant at a flow rate of 1 mL  $\text{min}^{-1}$  and different paint concentrations, such as 0.12–0.5 mg  $\text{mL}^{-1}$ . The filtration efficiency was measured in 1.5 mL intervals with UV-vis and AF-FFF. Measurement parameters for AF-FFF measurements are described in Tables S1 and S2 (Supporting Information).

#### 2.2.1. Filtration of Paint 1

The filtration efficiency for paint dispersions reached up to 100% for all used concentrations (**Figure 1A**), in contrast to the filtration efficiency of the paint supernatant. Here, the efficiency decreased over time (**Figure 1B**). These phenomena could also be observed from the filtrates (**Figure S1**, Supporting Information).

The pressure drop was recorded during the filtration experiments revealing an exponential increase after a certain filtration time (**Figure 2**). The elapsed time until the pressure increased was dependent on the paint concentration. However, no increase in pressure was detected during the filtration of paint 1 supernatant. The former observations can be explained by the different filtration mechanisms.

The filtration mechanism for paint 1 dispersion is size-exclusion. In the size-exclusion filtration, microparticles were separated on the top of the membrane resulting in a complete pore blockage. Therefore, the paint dispersion could not pass the membrane, which led to an increasing pressure drop. A conventional method to restore the membrane performance is the back-flushing method, where a washing fluid is pressed through the membrane in the opposite flow direction.

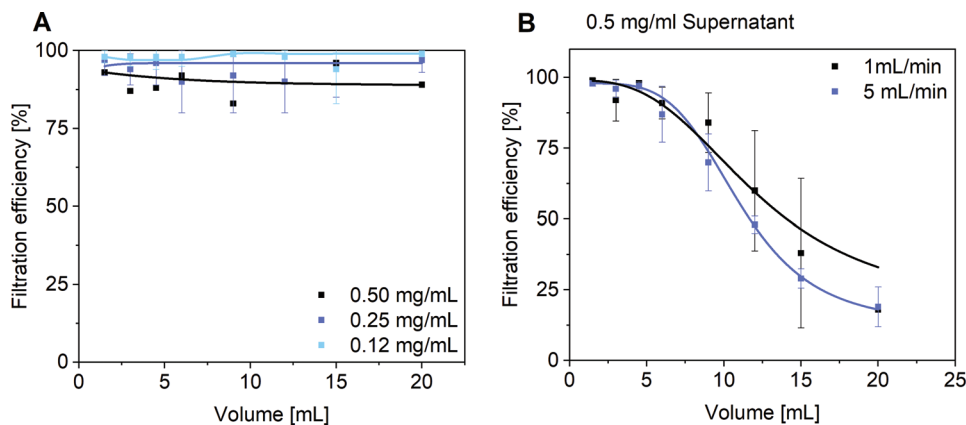


**Figure 1.** Filtration efficiency of paint 1 A) dependent on paint concentration and B) for paint supernatant dependent on the flow-rate. Filtration was done in triplicate with the diluted paint 1 (A) and the paint 1 supernatant received from centrifugation of paint 1 (B).

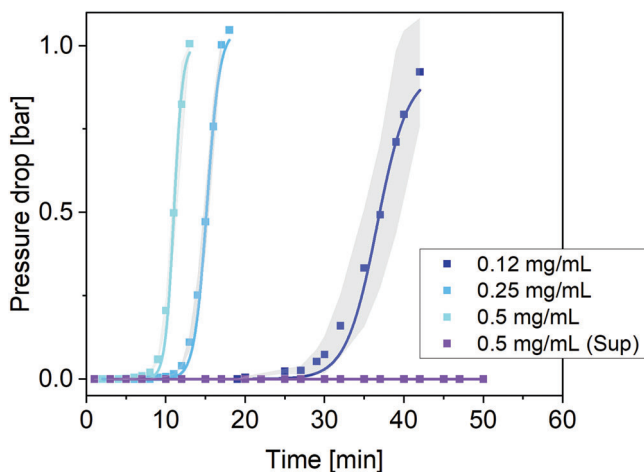


**Figure 2.** Pressure drop on the membrane at different paint concentrations for paint 1. Measurements were done in triplicate, the gray background marks the area of standard deviation.

The SEM images demonstrate the location of the three particle types of paint 1 on the fiber surface at low paint concentrations (**Figure 3A**). With ongoing filtration time, the amount of microparticles on the membrane surface was increased (**Figure 3B**) but nanosized, negatively charged titanium dioxide particles passed into the membrane bulk, where they were adsorbed on the fiber surfaces (**Figure 3C**).

In the second experiment, the paint 1 was separated by centrifugation (refer to Supporting Information for more details) and the supernatant was used for filtration experiments. The paint 1 supernatant did not contain nano or micro metal particles (**Figure 4A**) but only consisted of nanoplastic particles, which was proven by the SEM-BSD images. With the abundance of microparticles, no pore blockage, respectively, exponentially increasing pressure drop occurred. The nanoplastic particles passed through the membrane bulk, where they were adsorbed on the fibers (**Figure 4B,C**).

The second filtration mechanism, occurring at paint 1 supernatant filtration, is the affinity separation. The paint 1 super-

natant consists of polyacrylate nanoparticles, which possess a negative zeta potential measured in tap water caused by their surface functional groups. These negatively charged nanoplastics can then be adsorbed by the positively charged quaternary ammonium groups on the membrane surface due to electrostatic attraction. Since electrostatic forces are stronger than most other physical interactions, all nanoparticles, which come into contact with a free adsorption site on the membrane surface, while passing through the membrane, are strongly bonded to the quaternary ammonium groups located on the membrane surface. Thus, high filtration efficiencies can be reached and the strongly bonded nanoplastics are prevented from leaching out of the membrane with ongoing filtration time. However, with ongoing filtration time more and more adsorption sites are blocked and thus, also more and more nanoplastic particles can pass through the membrane without the required contact to a free adsorption site. This results in a decreasing filtration efficiency of the electrospun membrane and once all adsorption sites are blocked with nanoplastic particles, the maximum capacity of the membrane is reached and from that time on no following particles can be filtered.

This affinity mechanism demonstrates extraordinary properties, such as filtering particles smaller than the pore size at high filtration efficiencies with no pressure on the membrane. Thus, the affinity mechanism of these electrospun membranes, featuring high surface areas compared to conventional membranes, opens up unique possibilities in terms of nanoparticle filtration.

### 2.2.2. Filtration of Paint 2

Filtration experiments were also conducted for paint 2 and its supernatant. The filtration efficiency increased with rising paint concentration up to 100% during measurement time (**Figure 5A**). A high filtration efficiency becomes evident from the picture of filtrates, too (**Figure S2**, Supporting Information). However, the paint 2 supernatant demonstrated a low filtration efficiency of  $\approx 50\%$ , which was improved up to 80% by utilizing a higher membrane weight (**Figure 5B**). This improvement can be explained by the fact that a higher membrane weight correlates to more available adsorption sites for contaminant filtration. A similar effect

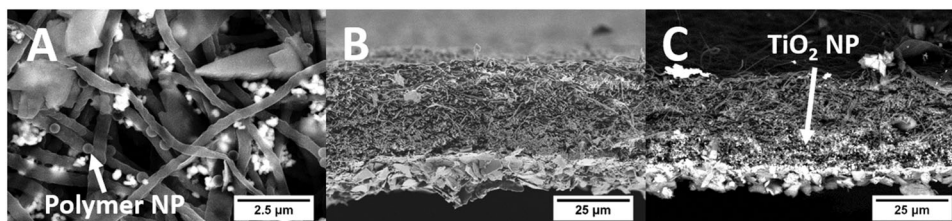


**Figure 3.** SEM images after filtration of paint 1. A) Top view with BSD detector, B) cross-section with SE2 detector, and C) cross-section with BSD detector.

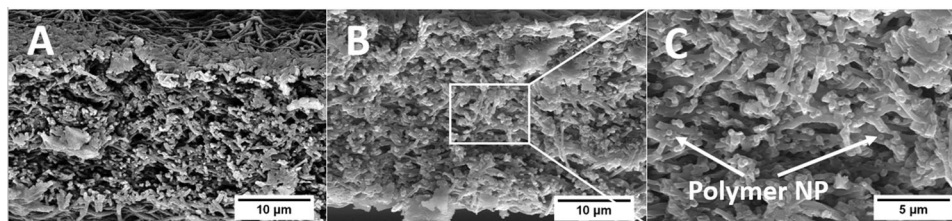


**Figure 4.** SEM cross-section images after filtration of paint 1 supernatant. A) Membrane with BSD detector, B) membrane with SE2 detector, and C) zoom-in of image (B).

can be achieved by reducing the used dispersion concentration of  $10 \text{ mg mL}^{-1}$  because a higher dispersion volume can then be filtered before capacity is reached. The capacity, which is defined as the ratio of adsorbed contaminant weight to the membrane weight, did not stabilize on a constant level but experiences a decline with increasing membrane weight.

The selection of the dispersion concentration was limited by the resolution of the measurement techniques, such as UV-vis. Thus, a higher concentration of paint 2 supernatant compared to paint 2 was utilized for filtration experiments. A higher or lower polymer concentration might not only change the ratio of membrane surface area to polymer concentration but also the polymer chain entanglement.

During the filtration process the increase in pressure was detected. The pressure drop increased not only for paint 2 but also for paint 2 supernatant. Filtration of paint 2 led to a pressure drop increase after a certain time (Figure 6A), in contrast to paint 2 supernatant, which provoked at nearly ten times higher test con-

centrations a rising pressure drop from the beginning onwards (Figure 6B). The continuously increasing pressure drop differentiates the filtration mechanism of paint 2 supernatant from others.

The filtration mechanism for paint 2 can be described as a size-exclusion type because microparticles block the membrane surface (Figure 7A). Since paint 2 supernatant did not contain particles but consisted of a dispersed copolymer, it can be supposed that it glued fibers and pores and thereby, blocked the membrane volume leading to the constantly rising pressure.

The dispersed copolymer contains acetate functional groups, which results in a strongly negative zeta potential at all pH values. Thus, we observe here again an electrostatic interaction between the dispersed polymer and the quaternary ammonium groups on the membrane surface. This enables successful filtration of the dispersed polymer but due to the high charge and high concentration affecting polymer chain entanglement of the dispersed polymer and the highly charged membrane surface, it might

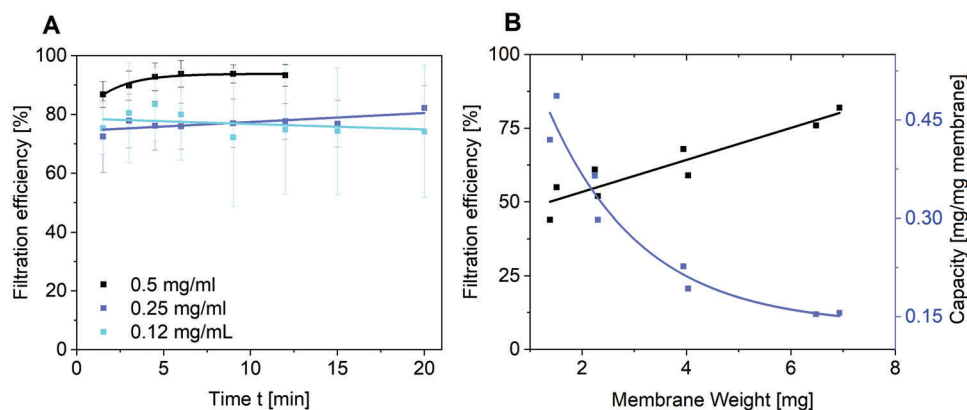


**Figure 5.** Filtration efficiency over time for A) paint 2 and B) paint 2 supernatant. Standard membrane weight is  $\approx 2.2 \text{ mg}$ .



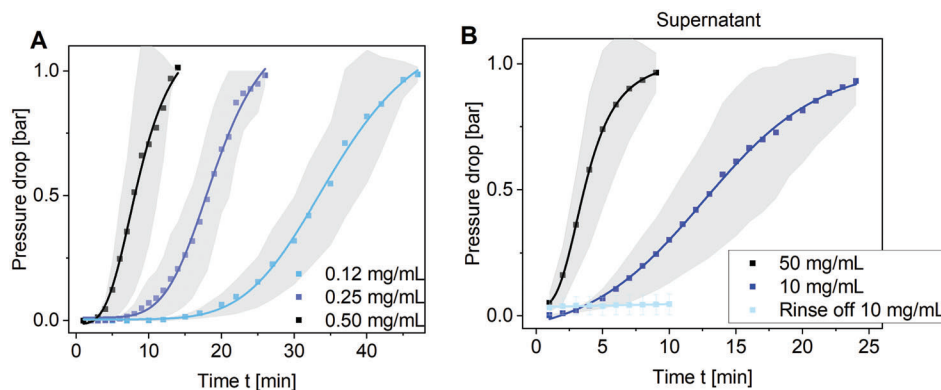


**Figure 6.** Pressure drop on the membrane at different paint concentrations for A) paint 2 and B) for paint 2 supernatant. Measurements were done in triplicate, the grey background marks the area of standard deviation.

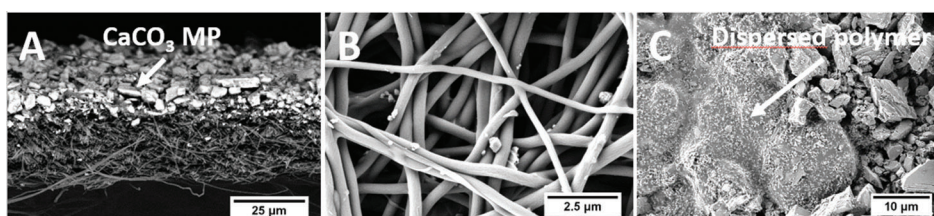


**Figure 7.** SEM images after filtration of paint 2. A) Membrane in cross-section with BSD detector, B) membrane top view with SE2 detector, and C) top view of membrane after filtration.

also cause a collective coagulation of more than just one layer of the polyelectrolyte on the membrane surface. And each polyelectrolyte can be expected to be in a voluminous, swollen state in aqueous media. The combination of these factors might also explain the expected pore blocking leading to the constantly increasing pressure on the membrane.

Although a pore blockage is expected, the dispersed polymer can hardly be seen on the dry membrane surface in SEM images (Figure 8A) only in some distinct areas fiber gluing can be observed (Figure 8B). However, its appearance can be recognized all over the filter area by a higher charge density in the SEM images (Figure 8C). The hypothesis of the even distribution of dispersed polymer in the membrane volume can be further evidenced by pictures of the membranes taken under UV irradiation (312 nm). These pictures show a higher reflection intensity in the inner membrane area, which was used for filtration (Figure S3D, Supporting Information).

The pore gluing by the dispersed polymer, which is assumed to be the driver for the increasing pressure drop can hardly be recognized on the membrane in the SEM images. An explanation can be the reversibility of the fiber gluing. Drying of the membranes after filtration might have led to ionomer type formation and, thus, opened the pores again. Therefore, SEM images demonstrate only fiber coating but no film formation. Further evidence was gained from a rinsing procedure. In this procedure, dried membranes from pressure drop tests were utilized, which have experienced a pressure drop of 1 bar at the end of the filtration experiment. These membranes were—after drying—again placed in the filtration apparatus and Milli-Q water can pass the filter at a pressure drop of roughly 0 bar (Figure 6B). Besides, no polymer was detected in the filtrate. Thus, pores were only

temporarily blocked during paint 2 supernatant filtration experiment.

The trade-off between a rising pressure on the membrane and the even distribution of contaminant in the membrane volume points out that the filtration of paint 2 supernatant can be described best by a combination of both mechanisms. The filtration of paint 2 supernatant fits the criteria of an affinity separation because negatively charged copolymers were attracted to the positively charged fibers and were not only filtered on the membrane surface but by depth filtration throughout the whole membrane volume. Additionally, the dispersed polymer might have glued the membranes pores, resulting in typical symptoms of size-exclusion filtration, such as rising pressure drop. However, it is expected, that a rising pressure on the membrane can be avoided and the filtration efficiency be increased by filtering lower concentrated polymer dispersions, which are supposed to feature less polymer chain entanglement.

The adsorption of contaminants, such as organic nanoparticles or dispersed polymers, on the membrane can also be understood as membrane fouling, which hinders membrane use for longer time periods. Either remediation strategies might be established or membranes can in future be designed as photocatalytic membranes.<sup>[38]</sup>

### 3. Conclusion

We have demonstrated the importance of noticing paints as a source for particle release with potential hazards to the environment. The release of paints into the environment, for example, by mechanical abrasion or in wastewater will result in a potential hazard for the environment and biota. Therefore, we propose a

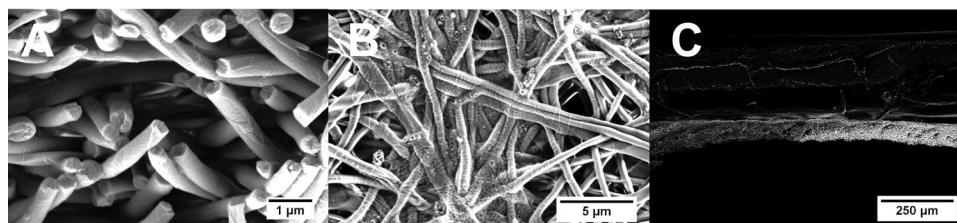


**Figure 8.** SEM images with SE2 detector after filtration of paint 2 supernatant A) in cross-section, B) top view, and C) zoom-out of figure (A).

feasible method to deal with this essential issue for water purification by membrane filtration process. Electrospun membranes successfully filtered particulate matter and dissolved materials with efficiencies up to 100%. The microparticles were filtered by size-exclusion mechanism in contrast to the titanium dioxide NPs, polyacrylate NPs, and the dispersed copolymers. Those contain charges on their surface, which enable electrostatic interaction with the membrane surface. Due to the electrostatic mechanism they can be filtered even though their size is smaller than the membrane pores and thus, no pore blocking occurs. Since they do not block membrane pores, they do not contribute to the pressure on the membrane at low concentrations, which are anyway more realistic to occur in the environment. This publication demonstrates the application of electrospun membranes for filtration of daily-life systems, which are composed of a mixture of different materials and evidenced the successful transfer of filtration principles from model NPs to daily-life systems.

## Supporting Information

Supporting Information is available from the Wiley Online Library or from the author.

## Acknowledgements

The authors gratefully acknowledge financial support from Bavarian State Ministry of the Environment and Consumer Protection (funding code TNT01NaT-72524) and the German Research Foundation, CRC 1357-“Mikroplastik” 391977956. Further thanks go to the KeyLab Electron and Optical Microscopy of the Bavarian Polymer Institute (BPI) for providing support and equipment for SEM measurements.

Open Access funding enabled and organized by Projekt DEAL.

## Conflict of Interest

The authors declare no conflict of interest.

## Data Availability Statement

The data that support the findings of this study are available in the supplementary material of this article.

## Keywords

affinity membranes, dispersed polymers, electrospun membranes, filtration, nanomaterials, paints

Received: April 6, 2022  
Revised: June 28, 2022  
Published online:

- [1] A. B. Sengul, E. Asmatulu, *Environ. Chem. Lett.* **2020**, *18*, 1659.
- [2] J. Gigault, A. T. Halle, M. Baudrimont, P.-Y. Pascal, F. Gauffre, T.-L. Phi, H. El Hadri, B. Grassl, S. Reynaud, *Environ. Pollut.* **2018**, *235*, 1030.
- [3] W. Wang, H. Gao, S. Jin, R. Li, G. Na, *Ecotoxicol. Environ. Saf.* **2019**, *173*, 110.
- [4] X.-D. Sun, X.-Z. Yuan, Y. Jia, L.-J. Feng, F.-P. Zhu, S.-S. Dong, J. Liu, X. Kong, H. Tian, J.-L. Duan, Z. Ding, S.-G. Wang, B. Xing, *Nat. Nanotechnol.* **2020**, *15*, 755.
- [5] V. S. Fringer, L. P. Fawcett, D. M. Mitrano, M. A. Maurer-Jones, *Front. Environ. Sci.* **2020**, *8*, <https://doi.org/10.3389/fenvs.2020.00097>
- [6] H. Gu, S. Wang, X. Wang, X. Yu, M. Hu, W. Huang, Y. Wang, *J. Hazard. Mater.* **2020**, *397*, 122773.
- [7] J. Hou, L. Wang, C. Wang, S. Zhang, H. Liu, S. Li, X. Wang, *J. Environ. Sci.* **2019**, *75*, 40.
- [8] D. Magri, P. Sánchez-Moreno, G. Caputo, F. Gatto, M. Veronesi, G. Bardi, T. Catelani, D. Guarnieri, A. Athanassiou, P. P. Pompa, D. Fragouli, *ACS Nano* **2018**, *12*, 7690.
- [9] L. Rubio, R. Marcos, A. Hernández, *J. Toxicol. Environ. Health* **2020**, *23*, 51.
- [10] K. Sawicki, M. Czajka, M. Matysiak-Kucharek, B. Fal, B. Drop, S. Męczyńska-Wielgosz, K. Sikorska, M. Kruszewski, L. Kapka-Skrzypczak, *Nanotechnol. Rev.* **2019**, *8*, 175.
- [11] M. Hu, D. Palić, *Redox Biol.* **2020**, *37*, 101620.
- [12] Z. Yu, Q. Li, J. Wang, Y. Yu, Y. Wang, Q. Zhou, P. Li, *Nanoscale Res. Lett.* **2020**, *15*, 115.
- [13] J. Wang, M. d. M. Nabi, S. K. Mohanty, A. N. Afroz, E. Cantando, N. Aich, M. Baalousha, *Chemosphere* **2020**, *248*, 126070.
- [14] S. Galafassi, L. Nizzetto, P. Volta, *Sci. Total Environ.* **2019**, *693*, 133499.
- [15] A. Turner, *Water Res.: X* **2021**, *12*, 100110.
- [16] D. M. Mitrano, S. Motellier, S. Clavaguera, B. Nowack, *Environ. Int.* **2015**, *77*, 132.
- [17] A. Cogulet, P. Blanchet, V. Landry, *Coatings* **2019**, *9*, 121.
- [18] M. J. Llana, M. S. Tolentino, N. C. C. Valeza, J. P. Reyes, B. A. Basilia, *IOP Conf. Ser.: Mater. Sci. Eng.* **2021**, *1117*, 012029.
- [19] A. Azimzada, J. M. Farner, I. Jreije, M. Hadioui, C. Liu-Kang, N. Tufekji, P. Shaw, K. J. Wilkinson, *Front. Environ. Sci.* **2020**, *8*, 2186.
- [20] A. Azimzada, J. M. Farner, M. Hadioui, C. Liu-Kang, I. Jreije, N. Tufekji, K. J. Wilkinson, *Environ. Sci.: Nano* **2020**, *7*, 139.
- [21] X. Zhang, M. Wang, S. Guo, Z. Zhang, H. Li, *J. Nanopart. Res.* **2017**, *19*, 374.
- [22] L. Sung, D. Stanley, J. M. Gorham, S. Rabb, X. Gu, L. L. Yu, T. Nguyen, *J. Coat. Technol. Res.* **2015**, *12*, 121.
- [23] R. Kaegi, A. Ulrich, B. Sinnet, R. Vonbank, A. Wichser, S. Zuleeg, H. Simmler, S. Brunner, H. Vonmont, M. Burkhardt, M. Boller, *Environ. Pollut.* **2008**, *156*, 233.
- [24] A. Van Wezel, I. Caris, S. A. E. Kools, *Environ. Toxicol. Chem.* **2016**, *35*, 1627.
- [25] C. C. Gaylarde, J. A. B. Neto, E. M. Da Fonseca, *Mar. Pollut. Bull.* **2021**, *162*, 111847.

- [26] G. Galli, E. Martinelli, *Macromol. Rapid Commun.* **2017**, *38*, 1600704.
- [27] P. Westerhoff, G. Song, K. Hristovski, M. A. Kiser, *J. Environ. Monit.* **2011**, *13*, 1195.
- [28] X. Wang, T. Han, Y. Sun, H. Geng, B. Li, H. Dai, *Environ. Pollut.* **2021**, *285*, 117408.
- [29] P. U. Iyare, S. K. Ouki, T. Bond, *Environ. Sci.: Water Res. Technol.* **2020**, *6*, 2664.
- [30] A. A. Horton, A. Walton, D. J. Spurgeon, E. Lahive, C. Svendsen, *Sci. Total Environ.* **2017**, *586*, 127.
- [31] D. P. Zagklis, P. G. Koutsoukos, C. A. Paraskeva, *Ind. Eng. Chem. Res.* **2012**, *51*, 15456.
- [32] S. Nair K, B. Manu, A. Azhoni, *J. Environ. Manage.* **2021**, *296*, 113105.
- [33] M. Malankowska, C. Echaide-Gorriz, J. Coronas, *Environ. Sci.: Water Res. Technol.* **2021**, *7*, 243.
- [34] R. Wang, L. Zhang, B. Chen, X. Zhu, *J. Membr. Sci.* **2020**, *614*, 118470.
- [35] A. Batool, S. Valiyaveetil, *J. Hazard. Mater.* **2021**, *413*, 125301.
- [36] Z. Uddin, F. Ahmad, T. Ullan, Y. Nawab, S. Ahmad, F. Azam, A. Rasheed, M. S. Zafar, *Int. J. Environ. Sci. Technol.* **2021**, *356*, 15.
- [37] A.-K. Müller, Z.-K. Xu, A. Greiner, *ACS Appl. Mater. Interfaces* **2021**, *13*, 15659.
- [38] A. M. Nasir, N. Awang, J. Jaafar, A. F. Ismail, M. H. D. Othman, M. A. Rahman, F. Aziz, M. A. Mat Yajid, *J. Water Process Eng.* **2021**, *40*, 101878.